A precession model explaining warped galaxies

Patricia Sánchez Martín

Joint work with J.J. Masdemont, M. Romero-Gomez

Universitat Ramon Llull

10 November 2016

Types of galaxies

Hubble's "tuning fork" diagram (from no disc to disc):

- Elliptical galaxies (E).
- Lenticular galaxies (S0).
- Spiral galaxies (S):
    - Normal spirals (Sa, Sb, Sc).
    - Barred spirals (SBa, SBb, SBc).
- Irregular galaxies (De Vaucouleurs).

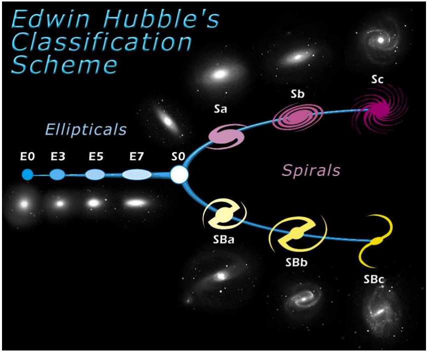

What is a warped galaxy?

From an edge-on point of view:

- **Warped galaxies**: the outer parts are not aligned with the inner plane of the disc.
- Classification by its shape:
  - **S-shaped** or grand-design warps (the most common).
  - U-shaped warps.
  - L-shaped or lopsided warps.

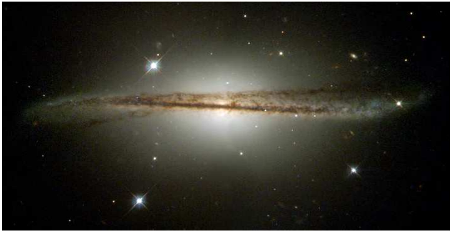

Galaxy ESO 510-G13 photographed by Hubble telescope.

S-Shaped warp U-Shaped warp L-Shaped warp

- Warped galaxies are a common phenomenon.
- But, the reason for this phenomenon is not known yet.
- Observed in the distribution of stars (Sánchez-Saavedra et al., 1990).
- Observed in the study of neutral hydrogen (Bosma, 1981).

Warped galaxies formation theories

A big amount of theories have been formulated in order to explain this warped shape. Some of them:

- Bending modes: Lynden-Bell (1965), Sparke & Casertano (1988), Revaz & Pfenniger (2004).
    - Binney et al. (1998): The inner halo would realign with the disc, and so the warp would dissipate.
- Misalignment of angular momenta:
    - By friction: Debattista & Sellwood (1999). Short-lived warps.
    - Accretion of material: Lopez-Corredoira et al. (2002), Read et al. (2008). Relation between warp angle and precession velocity unexplained.
- Tidal interaction: Levine et al. (2006).
    - But warps are just as common in isolated as in non-isolated galaxies.
- Sellwood (2013) determines that since warps are really common, they are either repeatedly regenerated or long-lived.

Our approach:

By means of dynamical system tools:

- **Purpose**: to use the invariant manifolds studying how they are affected by a precessing model acquiring the form of warps.
- Considering a **natural misalignment** between the angular momentum and the angular velocity, the resulting model is consistent and it is able to reproduce warped shapes.
- Line of our study: analysis of the invariant objects which cause in a similar dynamic way the formation of rings and spiral arms in barred galaxies (Romero-Gómez et al., 2006, 2007, Athanassoula et al., 2009).
- Invariant manifolds exist for as long as the potential does not change significantly. Thus warps are long-lived objects.

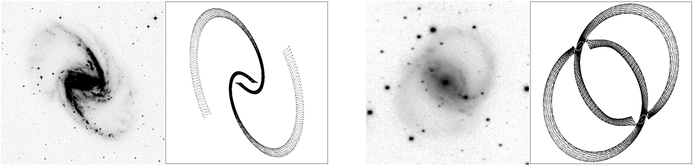

Athanassoula et al., 2009.

Components of the model

- An axysimmetric component modelled by a Miyamoto-Nagai disc potential:

$$\phi_d = -\frac{GM_d}{\sqrt{R^2 + (A + \sqrt{B^2 + z^2})^2}}$$

- A Plummer bulge or spheroid with potential ($A = 0$):

$$\phi_p = -\frac{GM_p}{\sqrt{r^2 + b^2}}$$

- A Ferrers bar with potential:

$$\phi_b = \pi\, G\, abc \frac{\rho_0}{n_h + 1} \int_\lambda^\infty \frac{du}{\sqrt{\Delta(u)}} (1 - m^2(u))^{(n_h+1)}$$

- **Gravitational potential**:
  - *First model*: $\phi = \phi_d + \phi_b$. $G(M_d + M_b) = 1$.
  - *Second model*: $\phi = \phi_d + \phi_b + \phi_p$. $G(M_d + M_b + M_p) = 1$.

Motion of the bar

- **Goal**: Effect of a small misalignment between the angular momentum and the angular velocity.
- Bar behaves as a rigid body.
- Angular momentum: $\mathbf{L} = \mathbf{I} \cdot \boldsymbol{\omega}$.
- No torque is applied to the bar.
- Axially symmetric bar along the x axis: $a > b = c$.

The body reference frame:

- Aligned with the main axes of the body.
- Inertia tensor:

$$\mathbf{I}_b = \begin{pmatrix} I_1 & 0 & 0 \\ 0 & I_2 & 0 \\ 0 & 0 & I_3 \end{pmatrix}$$

$I_1 = \frac{1}{5} M_b (b^2 + c^2)$, $I_2 = \frac{1}{5} M_b (a^2 + c^2)$, $I_3 = \frac{1}{5} M_b (a^2 + b^2)$.

- Angular velocity of the bar with respect to the static inertial axes, expressed in the body frame, $\boldsymbol{\omega}_b = (\omega_1, \omega_2, \omega_3)$.
- $\boldsymbol{\omega}_b$ is a solution of Euler's equations:

$$\begin{cases} I_1 \frac{d\omega_1}{dt} = \omega_2 \omega_3 (I_2 - I_3), \\ I_2 \frac{d\omega_2}{dt} = \omega_1 \omega_3 (I_3 - I_1), \\ I_3 \frac{d\omega_3}{dt} = \omega_1 \omega_2 (I_1 - I_2). \end{cases}$$

- $I_1 \neq I_2 = I_3$.
- ε: angle from the angular momentum $\mathbf{L}_b$ to the yz plane in the body reference. **Small**.
- Angular momentum in body reference:

$$\mathbf{L}_b = \begin{pmatrix} -L\sin(\varepsilon) \\ L\cos(\varepsilon)\sin(\lambda t) \\ L\cos(\varepsilon)\cos(\lambda t) \end{pmatrix}$$

$L = ||\mathbf{L}_b||$.

- Angular velocity in body reference:

$$\boldsymbol{\omega}_b = \begin{pmatrix} -\frac{L}{I_1}\sin(\varepsilon) \\ \frac{L}{I_T}\cos(\varepsilon)\sin(\lambda t) \\ \frac{L}{I_T}\cos(\varepsilon)\cos(\lambda t) \end{pmatrix}.$$

$\lambda = -\frac{I_T - I_1}{I_T}\frac{L}{I_1}\sin(\varepsilon) \approx -\frac{L}{I_1}\varepsilon$ precession rate (small).

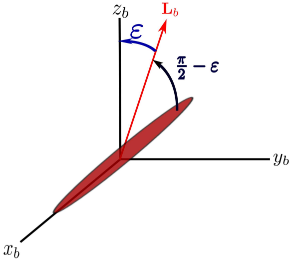

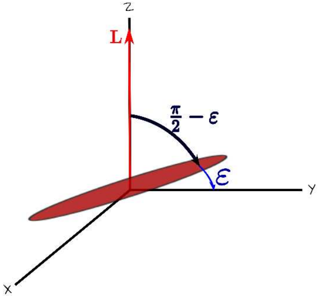

The precessing reference frame:

x axis aligned with the major axis of the bar. Bar rotating around the x axis.

- Rotation to the body reference:

$$R_p^b(t) = \begin{pmatrix} 1 & 0 & 0 \\ 0 & \cos(\lambda t) & -\sin(\lambda t) \\ 0 & \sin(\lambda t) & \cos(\lambda t) \end{pmatrix}.$$

- Angular velocity in precessing reference:

$$\boldsymbol{\omega}_p = R_p^b \cdot \boldsymbol{\omega}_b = \begin{pmatrix} -\frac{L}{I_1}\sin(\varepsilon) \\ 0 \\ \frac{L}{I_T}\cos(\varepsilon) \end{pmatrix}.$$

- Angular momentum in precessing reference:

$$\mathbf{L}_p = R_p^b \cdot \mathbf{L}_b = \begin{pmatrix} -L\sin(\varepsilon) \\ 0 \\ L\cos(\varepsilon) \end{pmatrix}.$$

- Angular velocity for the equations of motion:

$$\mathbf{\Omega_p} = \boldsymbol{\omega}_p + \begin{pmatrix} -\lambda \\ 0 \\ 0 \end{pmatrix}$$

ω_p=angular velocity of the body in the precessing frame.

$(-\lambda, 0, 0)$ = angular velocity of the precessing axes with respect to the body axes, expressed in the precessing frame.

$$\mathbf{\Omega_p} = \begin{pmatrix} -\Omega\sin(\varepsilon) \\ 0 \\ \Omega\cos(\varepsilon) \end{pmatrix}.$$

$$\Omega = ||\mathbf{\Omega_p}|| = \frac{L}{I_T} \text{ pattern speed.}$$

The precessing reference frame:

- Bar:
  - Main axis in the x axis of the precessing frame.
  - Rotates around the main axis with constant angular speed λ.
- Disc:
  - Placed in the xy plane of the precessing frame.
  - Static

The inertial reference frame:

- Bar:
  - Precesses around the Z axis (angular momentum).
  - Tilt angle ε with the XY plane.
- Disc:
  - Precesses following the bar.
  - Tilt angle ε with the XY plane.

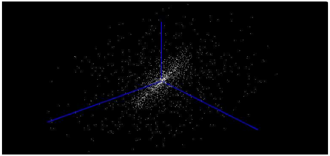

Equations of motion in the precessing reference frame

- Equation of motion of a particle in a non-inertial system:

$$\ddot{\mathbf{r}} = -\nabla\phi - 2(\mathbf{\Omega_p} \times \dot{\mathbf{r}}) - \mathbf{\Omega_p} \times (\mathbf{\Omega_p} \times \mathbf{r}), \text{ with } \mathbf{\Omega_p} = \begin{pmatrix} -\Omega \sin(\varepsilon) \\ 0 \\ \Omega \cos(\varepsilon) \end{pmatrix}.$$

- Equations of motion for the **precessing model**:

$$\begin{cases} \dot{x_1} = x_4 \\ \dot{x_2} = x_5 \\ \dot{x_3} = x_6 \\ \dot{x_4} = 2\Omega\cos(\varepsilon)x_5 + \Omega^2\cos^2(\varepsilon)x_1 + \Omega^2\sin(\varepsilon)\cos(\varepsilon)x_3 - \phi_{x_1} \\ \dot{x_5} = -2\Omega\cos(\varepsilon)x_4 - 2\Omega\sin(\varepsilon)x_6 + \Omega^2 x_2 - \phi_{x_2} \\ \dot{x_6} = 2\Omega\sin(\varepsilon)x_5 + \Omega^2\sin(\varepsilon)\cos(\varepsilon)x_1 + \Omega^2\sin^2(\varepsilon)x_3 - \phi_{x_3} \end{cases}$$

ε tilt angle, Ω modulus of the pattern speed, ϕ potential.

- Jacobi first integral given by,

$$\begin{aligned} C(x_1, x_2, x_3, x_4, x_5, x_6) = &- (x_4^2 + x_5^2 + x_6^2) + 2\Omega^2\sin(\varepsilon)\cos(\varepsilon)x_1x_3 \\ &+ (\Omega^2\cos^2(\varepsilon)x_1^2 + \Omega^2 x_2^2 + \Omega^2\sin^2(\varepsilon)x_3^2) - 2\phi, \end{aligned}$$

Basic structures of the precessing model

- ZVC: $\phi_{\text{eff}} > C$ forbidden regions for a star, where

$$\phi_{\text{eff}} = \phi - \frac{1}{2}\Omega^2(\cos(\varepsilon)^2 x^2 + y^2 + \sin(\varepsilon)^2 z^2) - \Omega^2 \sin(\varepsilon)\cos(\varepsilon) xz.$$

- Five Lagrangian equilibrium points:
  - L_3, L_4, L_5 maintain their coordinates fixed independently of ε.
  - L_1 and L_2 vary as ε changes.

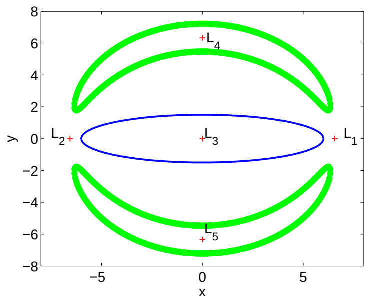

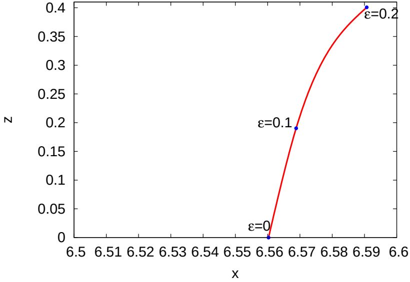

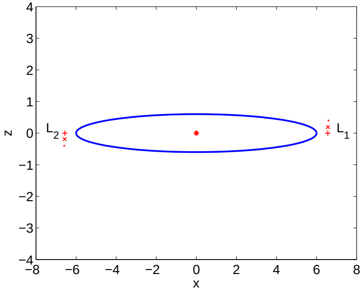

Periodic orbits around L_3

Model: Miyamoto-Nagai disc + Ferrers bar.

- Eigenvalues around L_3 $(\forall \varepsilon)$: $\{\lambda i, -\lambda i, \mu i, -\mu i, \omega i, -\omega i\}$ $(\lambda, \mu, \omega \in \mathbb{R}^+)$.
- L_3: linearly stable elliptic point.

Families of planar periodic orbits about L_3: stable and responsible for the skeleton of the bar's structure.

- $\varepsilon = 0$ model given by Pfenniger (1984).
- Change when ε varies, but the change is mostly in the *z* component.
- The *xy* projections remain essentially the same and they continue giving structure to the bar.
- Stability indexes: for a given value of ε, s_1 and s_2 cross the limits (± 2) an equal number of times and approximately at the same values of the energy.

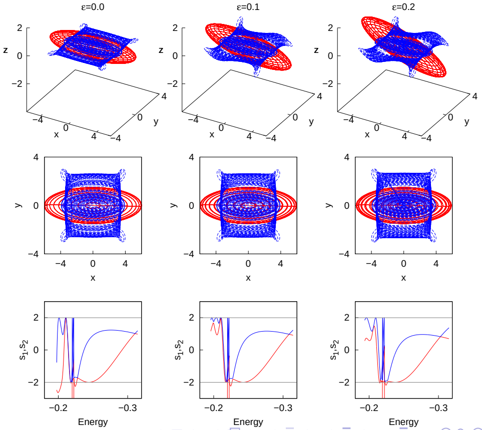

Dynamics close to corotation

Stability character of L_1 and L_2:

- Eigenvalues around L_1, L_2 ($\forall\varepsilon$): $\{\lambda, -\lambda, \mu i, -\mu i, \omega i, -\omega i\}$ (λ, μ, $\omega \in \mathbb{R}^+$).
- L_1, L_2: unstable hyperbolic points.
- Dynamics associated with the planar Lyapunov orbits.

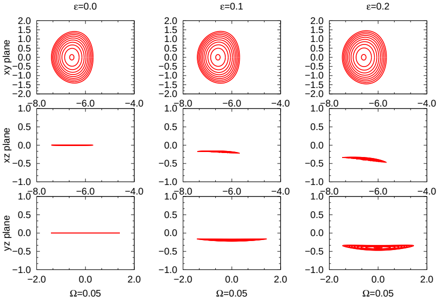

Lyapunov orbits around L_2

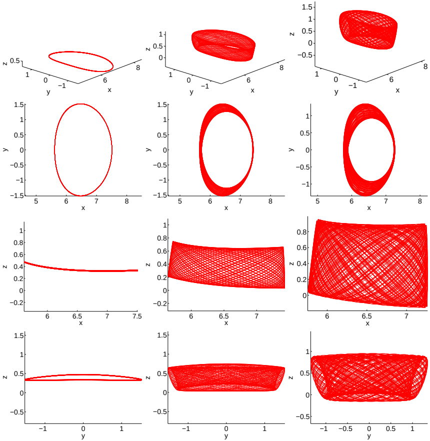

Lyapunov orbit, Lissajous orbits, Torus, around L_1 ($\varepsilon = 0.2$)

Role of the invariant manifolds:

- Trajectories outside the bar: responsible for the main visible building blocks. Responsible for the transport of matter.
- Associated to the unstable character of the libration point orbits about L_1 and L_2.

- The set of these orbits: Trajectories that are assymptotic to the Lyapunov periodic orbit.
  - Forward in time (*stable manifold*):

$$W^s_{loc}(\gamma) = \left\{ X \in \mathbb{R}^6 | \lim_{t \to \infty} ||\mathbf{\Psi}(t, X) - \gamma|| = 0 \right\}.$$

  - Backwards in time (*unstable manifold*):

$$W^u_{loc}(\gamma) = \left\{ X \in \mathbb{R}^6 | \lim_{t \to -\infty} ||\mathbf{\Psi}(t, X) - \gamma|| = 0 \right\}.$$

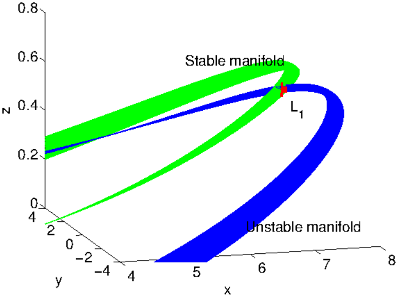

Invariant manifolds give rise to external structures:

- Invariant manifolds of Lyapunov orbits around the equilibrium points, L_1 and L_2: vary with the tilt of the model, the angular velocity or the bar mass.
- The structure of the invariant manifolds is preserved for different values of ε, but with slight peculiarities.
- The position of the invariant manifolds is not exactly the same in the three columns for a given value of GM_b. z-component also increases in absolute value.
- The structure remains but the spiral arms slowly open up. Moreover, when the bar mass increases, the structure moves from a morphology of a rR_1 ringed galaxy to that one of a spiral galaxy.
- Morphologies: Precessing model does not change the morphology expected from previous studies.

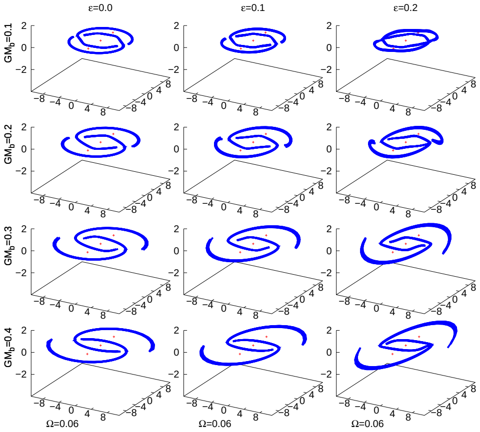

$GM_d \in [0.6, 0.9]$, $GM_b \in [0.1, 0.4]$, $\Omega = 0.06$. Tilt angle $\varepsilon \in [0, 0.2]$.

Evidence of warps

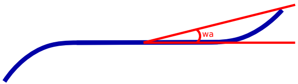

- $\varepsilon = 0$: No warped shape, as expected.
- $\varepsilon > 0$: Warped outer branches of the unstable manifold.
  - GM_b increases: warp S-shape more evident. Increase warp angle.
  - Contribution of the inner branches of the manifolds.

ε	Ω	GM_b	wa ($^\circ$)
0.1	0.05	0.1 - 0.4	1.8 - 3.9
0.1	0.06	0.1 - 0.4	1.8 - 4.8
0.2	0.05	0.1 - 0.4	3.8 - 7.7
0.2	0.06	0.1 - 0.4	3.7 - 9.3

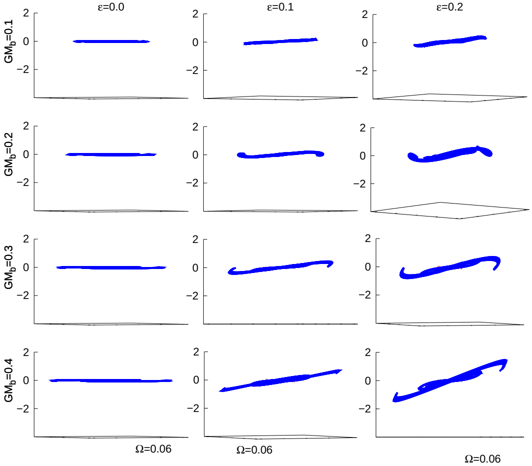

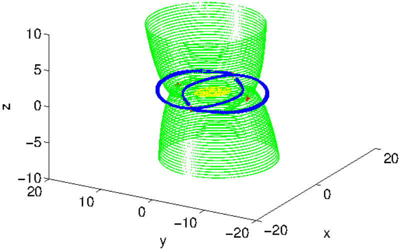

Invariant manifold (blue), zero velocity surface (green) and Ferrers bar (yellow).

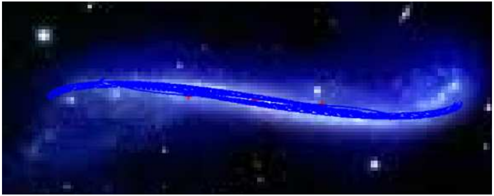

Warp obtained with the parameters $\varepsilon = 0.2, \Omega = 0.05$ and $GM_b = 0.3$ (blue) superimposed to the Integral Sign Galaxy, UGC 3697.

Test particle simulations

- Zero dispersion in the initial conditions.

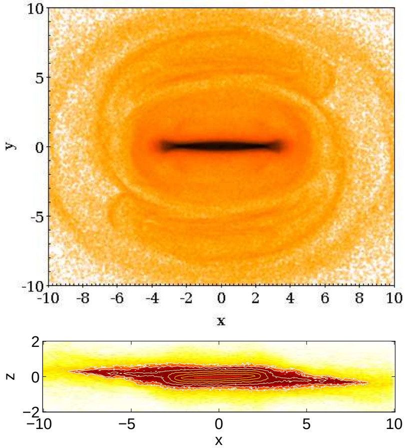

Top: Surface density of the xy-projection.
Bottom: Surface density and contours of the xz-projection. $GM_d = 0.7$, $GM_b = 0.3$, $\Omega = 0.05$, $\varepsilon = 0.2$ rad

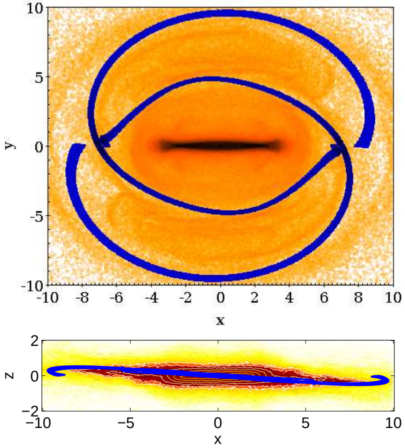

Overlap of the invariant manifolds

Warp angles

ε	Ω	GM_b	θ (°)
0.1	0.05	0.1 - 0.4	1.8 - 3.9
0.1	0.06	0.1 - 0.4	1.8 - 4.8
0.2	0.05	0.1 - 0.4	3.8 - 7.7
0.2	0.06	0.1 - 0.4	3.7 - 9.3

Warp angles θ (in degrees) obtained in the precessing disc and bar model.

Model	ε	GM_p	GM_b	θ (°)
A	0.1	0.5	0.1	7.3
B	0.1	0.4	0.1	4.9
C	0.1	0.3	0.2	5.2
D	0.1	0.2	0.2	5.0

Model	ε	GM_p	GM_b	θ (°)
A	0.2	0.5	0.1	12.3
B	0.2	0.4	0.1	6.3
C	0.2	0.3	0.2	9.9
D	0.2	0.2	0.2	9.8

Warp angles θ (in degrees) obtained in the precessing model with halo. $\Omega = 0.06$.

Model	ε	Ω	GM_p	θ (°)
A'	0.1	0.06	0.4	5.7
B'	0.1	0.06	0.3	5.2
C'	0.1	0.06	0.2	4.8
D'	0.1	0.06	0.1	4.5

Model	ε	Ω	GM_p	θ (°)
A'	0.2	0.06	0.4	11.3
B'	0.2	0.06	0.3	10.4
C'	0.2	0.06	0.2	9.6
D'	0.2	0.06	0.1	8.9

Warp angles θ (in degrees) obtained in the precessing model with halo when the bar mass is fixed to $GM_b = 0.3$.

Conclusions

- A precessing model explains the formation of warped galaxies in agreement with observations.
- The precession is produced in a natural way in barred galaxies, and is in fact the generic behaviour.
  - The formation of the bar from the disc causes the precession.
  - This precession arises through a misalignment between the angular momentum and angular velocity.
- This precession is an explanation of the maximal observed size of warp angles.
- The presence of a halo favours larger warp angles.
- The warped shape is induced by the invariant manifolds of the system.

** P. Sánchez-Martín, M. Romero-Gómez, J. Masdemont, Warp evidences in precessing galactic bar models, A&A, 588, A76 (2016)*

Future work

- Verify with N-body simulations the results of our model.

- Explain U-shaped and L-shaped warps:

S-Shaped warp U-Shaped warp L-Shaped warp

  - Are they due to a non-homogeneous bar density?
  - Or to the velocity of the bar differing from that of the disc? (non-autonomous problem)
  - Or do they only appear in non-isolated galaxies and are due to interactions between galaxies?